Shape and size of non-spherical silver nanoparticles: implications for calculating nanoparticle number concentrations

Christopher A. Little, Christopher Batchelor-McAuley, Neil P. Young, and Richard G. Compton*

* corresponding author: Prof. Dr. Richard G. Compton, Department of Chemistry, Physical & Theoretical Chemistry Laboratory, Oxford University, South Parks Road, Oxford, OX1 3QZ, United Kingdom

Email: richard.compton@chem.ox.ac.uk Tel: +44(0)1865275957 Fax: +44(0)1865275410

Abstract:

The international drive to measure accurate number concentrations of nanoparticles is impeded by the typically heterogeneous populations of non-spherical nanoparticles. The irregular shape and size of "50 nm" silver nanoparticles is studied using Electron Tomography. It is evidenced that even for highly symmetrical particles the volume can be over 20% less than that of the circumscribed sphere; more irregularly shaped particles can have volumes of over 45% less. On this basis, criteria are provided to determine the particle sphericity from 2D projections obtained from Electron Microscopy, including an empirical method for particle volume estimation. The results allow the visualisation of irregularly shaped particles, revealing the presence of previously unseen voids in the nanoparticle structure. Comparison of tomographic data with other commonly used particle-sizing methods exposes the limitations of these methods in studying nanoparticle populations that exhibit heterogeneity.

Main Text:

The size, shape and volume of nanoparticles (NPs) are critical parameters when considering their reactivity, toxicity and optical properties.[1–3] However, NP populations are necessarily heterogeneous; commercially synthesised nominally spherical NPs of the same diameter can exhibit a large degree of heterogeneity in size and shape. For example, the gold NP standard reference materials provided by the National Institute of Standards and Technology (NIST) show a clear variation in morphology.[4] In a 2011 EU recommendation, nanomaterials are defined in terms of the median number-weighted size distribution.[5,6] Equally, measuring the NP *number concentration* is of direct relevance in industries including pharmaceuticals and cosmetics. Accurately measuring a NP number concentration is experimentally challenging; state-of-the-art research aims to develop traceable methods for measuring number concentrations to within a 10% error.[7] Broadly, estimation of the NP number concentration is

often achieved by dividing the total concentration of the material by the amount of material per NP, a method heavily reliant on an *accurate* value of the average amount of material per NP, the measure of which is sensitive to its size, shape and density. An essential question is how big an error does the assumption that NPs are spherical lead to in defining the number concentration?

For most NPs it is widely assumed that the density is comparable to that in the bulk metal; even for NPs of 5 nm diameter the lattice parameters are commonly within 1% of the bulk value.[8] However, it is more difficult to define the NP shape, size and associated distributions. Commonly used NP sizing techniques such as Dynamic Light Scattering (DLS) and Nanoparticle Tracking Analysis (NTA) neglect shape information entirely by detecting the hydrodynamic radii based on the equivalent sphere. These radii often appear much larger than the geometric radii measured by electron microscopy, depending on the NP capping agent.[9] Challengingly, inter-laboratory studies have reported significant variations in size even when using the same equipment.[10–12] Any error in the measured radius will lead to a cubic error in estimated NP volume.

Of the presently available NP characterisation techniques, Transmission Electron Microscopy (TEM) has the best resolution in defining NP shape. However, the interpretation of 2D projections to obtain a 3D volume estimate is complex. For NP samples that exhibit heterogeneity in morphology, the attainment of an accurate volume distribution has required significant approximations to be made regarding the NP geometry.[13,14] Whilst a recent study presented an efficient method for determining NP volumes through the combined use of SEM and AFM,[15] tomography is required for truly accurate 3D shape *and* volume determination. Tomography has progressed significantly following the postulation of its mathematical basis in 1917.[16] Whilst initially developed for biological imaging,[17] improvements in TEM-based *Electron* Tomography (ET) have enabled 1 nm resolution in 3D[18,19] and recently allowed the reconstruction of one *ca.* 10 nm gold NP at a resolution of 2.4 Å.[20] However, such advances have yet to be applied to the determination of size or volume *distributions*, particularly for irregularly shaped NPs. In ET, TEM images are recorded about a tilt axis, before the ensemble of images are 'back-projected' to give a 3D reconstruction.[21] This provides shape, size, *and* volume information, allowing the accurate calculation of NP number concentrations without introducing the errors inherent in the use of other NP sizing techniques.

This work studies irregular, non-spherical "50 nm" silver NPs. ET is used to estimate their 3D volumes. From these reconstructions the question of how accurately can the NP size distribution be estimated from 2D imaging is approached. We find that even for relatively symmetrical NPs the volume can be over 20% smaller than that of the circumscribed sphere,

whilst more irregularly shaped particles can have volumes of over 45% less than this sphere. The ET calculated volumes are then used to establish a set of empirical correction factors that can be used to estimate accurate NP volumes from 2D TEM images. Comparing the size information from ET with that obtained from other commonly used NP sizing techniques demonstrates the severe limitations of these other techniques in calculating NP volumes and hence NP number concentrations.

The dual-axis tilt-series of a sample of silver NPs (nominally "50 nm diameter", NanoXact, Nanocomposix, USA) were reconstructed to give tomograms. An example of a tomogram image is presented in the SI section S2. The NPs were segmented and binarised to give a series of *z*-stack images for 13 NPs. The processes involved are detailed in the SI section S3. Examples of 3 3D-rendered NPs are presented in Figure 1. Here the z-axis corresponds to the axis of observation for the non-tilted sample and the x and y coordinates are arbitrarily assigned. The thermodynamically equilibrated shape of NPs of this size has been calculated to be that of a truncated octahedron.[22] However, whilst the NPs exhibit a degree of irregular surface structure, they are not faceted in this way and lack symmetry. This can likely be related to the growth of the NPs occurring during synthesis *via* chemical reduction of Ag(I) salts under kinetic control, leading to shapes of low symmetry.

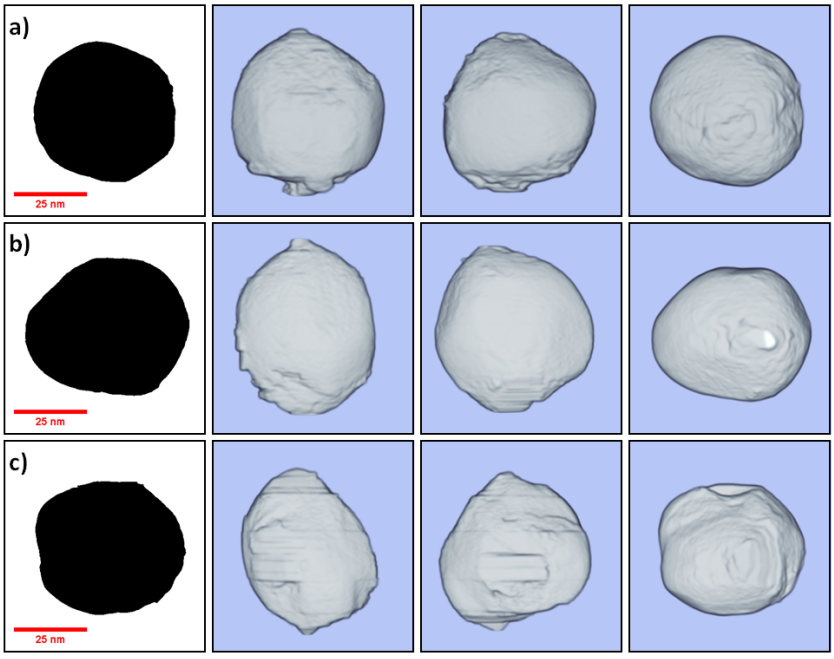

Figure 1. 2D binary projections of 3 *ca.* 50 nm silver NPs viewed down the *z* axis (left) and 3D images rendered in Tomviz 1.3.0,[23] as viewed down the *x*, *y* and *z* axes (right) from left to right.

Multiple features are evident in the reconstructed *z*-stacked tomogram images (SI section S2) seen as light regions of *ca.* 2 nm diameter against the dark NP background. Examples of such

regions are presented in the SI section S4, and a video is available online depicting these features frame by frame at 10 fps through the *z*-stack of a NP. These features are not artefacts of the reconstruction; they are present in the single reconstructions for both perpendicular tilt-series (the final reconstruction combines the two) and they show negligible translation in the *x*-*y* plane as a function of the *z* coordinate. Consequently, these regions likely correspond to voids in the NP, likely arising during the growth stage of NP synthesis. At present it has not been possible to identify if these voids are empty or simply filled with a relatively low electron scattering material. By approximating these voids as spheres, their volumes can be calculated; for one NP, 44 voids were identified with an average diameter of 2.58 ± 0.20 nm. This NP consists of *ca.* 3.4×10^6 Ag atoms, with on average *ca.* 900 Ag atoms per void; corresponding to *ca.* 1.1% of the total NP volume. The percentage error of the total volume that these voids make up is, in the present case, small but not insignificant; for other samples the presence of such voids in their structure may lead to an appreciable error in the number concentration estimate.

The volume of each NP was calculated (see SI section S1), affording the distribution presented in Figure 2 (blue line). Using these volumes, a series of correction factors can be established to allow a precise estimate of the nanoparticle volume from its 2D projection, as would normally be recorded in standard TEM imaging. These correction factors were obtained by taking 2D projections of the reconstructed NPs as viewed down the *z* axis (see Figure 1) and using the ratio of the maximum and minimum Feret diameters as a measure of the particles circularity in the 2D projection; a Feret diameter is the distance between two parallel tangents of the 2D outline of a NP shape.[24,25] The circumscribed volume was calculated from the maximum Feret diameter and compared to the tomographic volumes, giving the exact correction factor for each NP. Calculating the ratio of the maximum to minimum Feret diameter (the Feret ratio) divided the 13 NPs into 3 distinct classes. This data and the associated mean correction factors for each class are presented in Table 1.

Feret Ratio	NPs	Correction Factor
1.0 – 1.1	4	0.779 ± 0.035
1.1 – 1.2	4	0.760 ± 0.017
1.2 – 1.4	5	0.653 ± 0.039

Table 1. Classification of silver NPs by Feret ratio with associated mean correction factors. As a note of caution these means and standard deviation are provided on the basis of a relatively small sample size.

Strikingly, this result indicates that even NPs that appear almost circular in 2D (*i.e.* have a Feret ratio of 1.0-1.1) can have a volume of over 20% less than that of the circumscribed sphere. The decrease in volume as a result of the divergence of polyhedral motifs from the circumscribed

sphere is well documented; atomic-scale fine structure can lead to further divergence from these ideal polyhedra.[26] Given the similarity between the correction factors for the NPs with a Feret ratio of 1.0-1.2, correction factors of 0.77 and 0.65 were determined for NPs in the ranges 1.0-1.2 and 1.2-1.4 respectively. The volume distributions obtained from ET and using this method are presented in the SI section S5. There is an excellent agreement between the distributions; the mean volumes calculated from ET and from the projections are 7.61 ± 0.47 × 10^{-23} m^3 and 7.65 ± 0.49 × 10^{-23} m^3 respectively, an error of *ca*. 0.5%.

An alternative method to obtain a 3D volume estimate from a 2D NP projection is to calculate the radius of a circle of equivalent area of the NP projection and calculate the spherical volume based on this radius. This method results in an excellent agreement between the volume distributions reconstructed by this method and by ET; these results are presented in the SI section S6. The mean volume obtained by this method is 7.87 ± 0.45 × 10^{-23} m^3, an overestimation of the volume by 3.5%. Given that this method is independent of the ET study (the method above required optimisation of correction factors by comparison with the ET data), this has a more general application. This overestimation of 3.5% is an estimate of the *minimum* error to which the NP volume and hence number concentration can be measured without recourse to ET.[27]

NTA and DLS measurements were performed on the NP suspensions. The distribution obtained from DLS is the intensity distribution; this can be weighted to obtain a number or volume distribution, however this can introduce a significant error into the measured distribution. DLS and NTA measurements take the form of a distribution of *radii*; several essential observations must be highlighted. First, a severe limitation of these two methods is the inherent assumption that the NPs are spherical when calculating radii on the basis of the Stokes-Einstein equation. It was demonstrated above that even NPs that appear quasi-spherical in 2D (i.e. have a Feret ratio of 1.0-1.1) can have a volume of over 20% less than that of the circumscribed sphere. Furthermore, comparison of this data with that obtained from TEM and ET requires transformation of the data from the latter two methods. Finally, DLS and NTA measurements calculate a *hydrodynamic* radius as opposed to the *geometric* radius calculated from TEM, leading to a larger measured radius.

Having ascertained optimised correction factors (as outlined in Table 1 for this NP sample) for use in obtaining 3D volumes from TEM images, these can be applied to a larger sample of TEM data. Using the optimised correction factors developed above, TEM images of 89 silver NPs were analysed to afford a volume distribution; representative TEM images are presented in the SI section S7. To compare the volumes calculated from TEM and ET with the radii obtained from

DLS and NTA, the effective radii of a sphere of equivalent volume were calculated. The resulting effective radii distributions are presented in Figure 2 with the hydrodynamic radii distributions from DLS and NTA overlaid, the effective radii distribution calculated from TEM with no correction factor applied is also plotted for comparison.

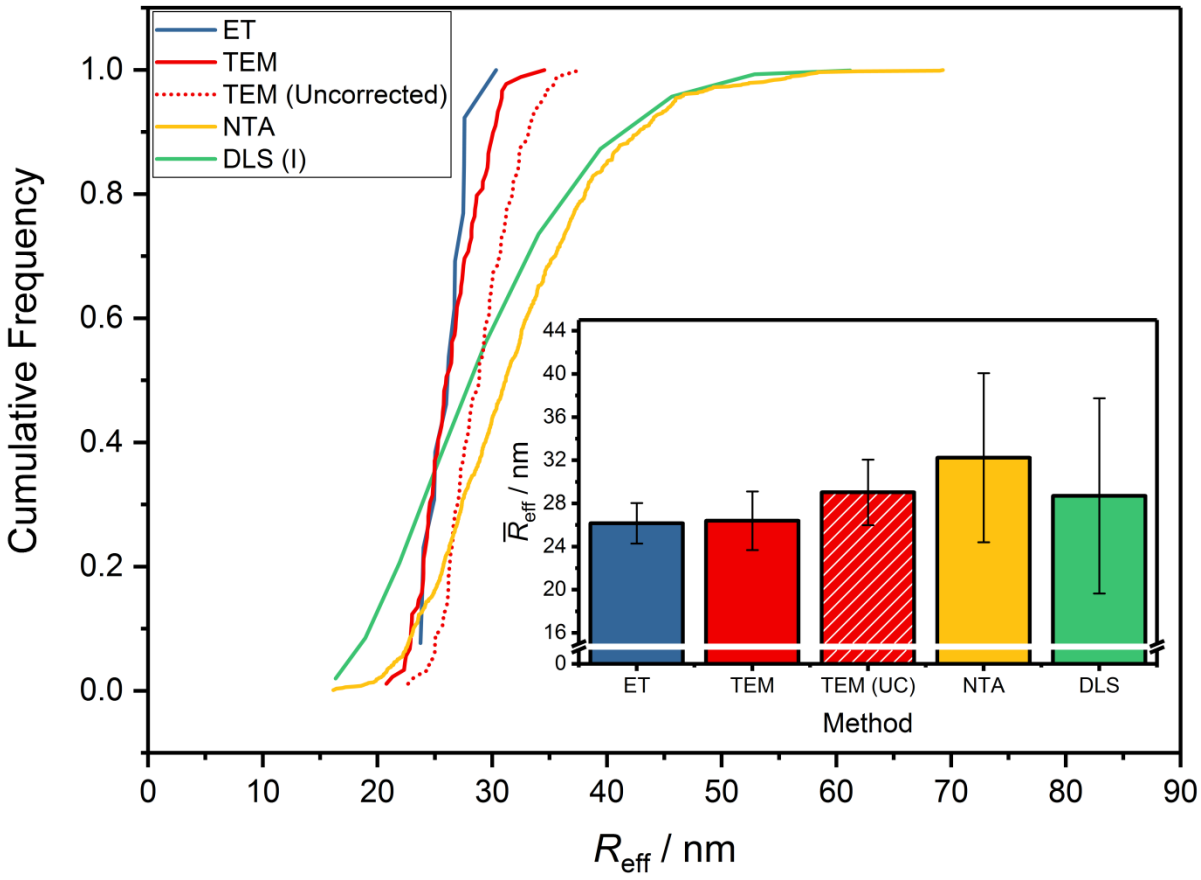

Figure 2. Cumulative frequency effective radii distribution for silver NPs as calculated *via* ET (blue line), TEM (with optimised correction factors, red line), TEM (uncorrected, dotted red line) with the hydrodynamic radii calculated from NTA (yellow line) and DLS (green line) overlaid. Inlay depicts the mean radii and standard deviation for the 5 methods.

This comparison is multiply insightful. First, it is strikingly evident from the distributions in Figure 2 that, as expected, both NTA and DLS dramatically overestimate the distribution width.[28,29] Whilst the distributions for these two methods are comparable, they predict mean radii of 32.24 and 28.71 nm respectively, *ca.* 23% and 10% larger than that predicted by ET respectively. Given that the error in radius is proportional to the cubic error in volume, this will result in a significant volume overestimation. Second, the optimised correction factors calculated in the previous section have a substantial effect on the mean effective NP radius calculated from TEM. Before their application, the mean radius is overestimated by *ca.* 11% compared to ET, but this decreases to within 1% of the ET value following their application. The

distribution widths calculated by ET and TEM are comparable and are significantly narrower than those from NTA and DLS. From the DLS measurements, a polydispersity index (PdI) of 0.084 was obtained, indicating a narrow distribution.[30] In spite of this, the significant width compared to the ET and TEM distributions is indicative of the deficiencies of DLS as a NP sizing technique; this is further discussed in the SI section S8. Given the loss of any *shape* information and the overestimation of both the mean radius of the NPs *and* the distribution width, the limitations of DLS and NTA are patently clear for NP populations that exhibit heterogeneity. Consequently, if the nanoparticle number concentration is to be determined from knowledge of the particle volume it is preferable to use a technique that is capable of *directly* measuring the particle volume; the errors associated with the assumption of the material's density being equal to that of the bulk are relatively minimal. In the present case, the effective density of the material is only decreased by approximately 1.1% by the presence of the voids and the particles are sufficiently large (>5 nm) that changes to the lattice structure are likely non influential. However, due to the lack of techniques available and the inherent difficulty in measuring particle volumes it is concluded that the optimal route to measuring nanoparticle number concentration is likely through the use of techniques capable of stochastically 'counting' the number of particles present in a given sample volume.

ET has facilitated the 3D reconstruction of nominally spherical silver NPs, revealing the substantial heterogeneity and irregularity in their shape, as well as the presence of small voids in their structure. It has been demonstrated that even the more highly symmetrical NPs can have a volume of over 20% less than that of the circumscribed sphere, whilst more irregularly shaped particles can have volumes of over 45% less than this sphere. Comparison of the NP size distributions with those determined by commonly used NP sizing techniques such as DLS and NTA has highlighted the tendencies of these techniques to vastly overestimate the NP size and size distribution. Whilst the error introduced by the presence of voids in the NP structure is fairly insignificant in the present work, when compounded by the errors in the determination of NP size from TEM data and the subsequent volume estimations, we conclude that it is likely that calculations of NP number concentrations to within a 5% error are unattainable by volume-based methods.

Acknowledgement

This work is supported by funding from the ERC under the EU's Seventh Framework Programme (FP/2007-2013)/ERC Grant Agreement no. 320403.

The authors thank Dr Errin Johnson and Dr Adam Costin for tomogram acquisition.

Keywords

Electron Microscopy, Nanoparticles, Number Concentrations, Particle Sizing, Tomography

References

[1] A. Albanese, P. S. Tang, W. C. W. Chan, *Annu. Rev. Biomed. Eng.* **2012**, *14*, 1–16.

[2] A. Nel, T. Xia, L. Mädler, N. Li, *Science* **2006**, *311*, 622–627.

[3] L. Kelly, E. Coronado, L. L. Zhao, G. C. Schatz, *J. Phys. Chem. B* **2003**, *107*, 668–677.

[4] S. B. Rice, C. Chan, S. C. Brown, P. Eschbach, L. Han, D. S. Ensor, A. B. Stefaniak, J. Bonevich, A. E. Vladár, A. R. Hight Walker, et al., *Metrologia* **2013**, *50*, 663–678.

[5] T. Linsinger, G. Roebben, D. Gilliland, *Requirements on Measurements for the Implementation of the European Commission Definition of the Term "Nanomaterial,"* Publications Office Of The European Union, **2012**.

[6] Commission Recommendation of 18 October 2011 on the Definition of Nanomaterial, *Offical Journal of the European Union* **2011**, 2011/696/EU.

[7] "Work Package 1: Particle Number Concentration," can be found under http://empir.npl.co.uk/innanopart/results/work-package-1-particle-number-concentration/, **2011**.

[8] W. H. Qi, M. P. Wang, *J. Nanoparticle Res.* **2005**, *7*, 51–57.

[9] E. E. L. Tanner, S. V. Sokolov, N. P. Young, C. Batchelor-McAuley, R. G. Compton, *Angew. Chem. Int. Ed.* **2017**, *56*, 12751–12754.

[10] C. Y. Wang, W. E. Fu, H. L. Lin, G. S. Peng, *Meas. Sci. Technol.* **2007**, *18*, 487–495.

[11] P. Hole, K. Sillence, C. Hannell, C. M. Maguire, M. Roesslein, G. Suarez, S. Capracotta, Z. Magdolenova, L. Horev-Azaria, A. Dybowska, et al., *J. Nanoparticle Res.* **2013**, *15*, 2101–2112.

[12] D. Langevin, O. Lozano, A. Salvati, V. Kestens, M. Monopoli, E. Raspaud, S. Mariot, A. Salonen, S. Thomas, M. Driessen, et al., *NanoImpact* **2018**, *10*, 97–107.

[13] C. A. Little, R. Xie, C. Batchelor-McAuley, E. Katelhon, X. Li, N. P. Young, R. G. Compton, *Phys. Chem. Chem. Phys.* **2018**, *20*, 13537–13546.

[14] S. V. Sokolov, C. Batchelor-McAuley, K. Tschulik, S. Fletcher, R. G. Compton, *Chem. Eur. J.*

2015, *21*, 10741–10746.

[15] R. Attota, E. C. Liu, *Anal. Bioanal. Chem.* **2016**, *408*, 7897–7903.

[16] J. Radon, *Akad. Wiss.* **1917**, *69*, 262–277.

[17] J. Frank, *Electron Tomography : Methods for Three-Dimensional Visualization of Structures in the Cell*, Springer, **2006**.

[18] I. Arslan, T. J. V Yates, N. D. Browning, P. A. Midgley, *Science* **2005**, *309*, 2195–2198.

[19] J. M. Thomas, P. A. Midgley, C. Ducati, R. K. Leary, *Prog. Nat. Sci. Mater. Int.* **2013**, *23*, 222–234.

[20] M. C. Scott, C.-C. Chen, M. Mecklenburg, C. Zhu, R. Xu, P. Ercius, U. Dahmen, B. C. Regan, J. Miao, *Nature* **2012**, *483*, 444–447.

[21] P. A. Midgley, R. E. Dunin-Borkowski, *Nat. Mater.* **2009**, *8*, 271–280.

[22] A. L. González, C. Noguez, J. Beránek, A. S. Barnard, *J. Phys. Chem. C* **2014**, *118*, 9128–9136.

[23] M. D. Hanwell, U. Ayachit, D. A. Muller, R. Hovden, "The Tomviz Project," can be found under https://tomviz.org/, **2018**.

[24] H. G. Merkus, *Particle Size Measurements: Fundamentals, Practice, Quality*, Springer Netherlands, **2009**.

[25] L. R. Feret, *Congrès Zurich, Assoc. Int. Pour l'Essai Des Matériaux* **1932**, *2*, 428–36.

[26] A. D. Banadaki, S. Patala, *npj Comput. Mater.* **2017**, *3*, 13.

[27] This error is likely an underestimation; the digital image resolution is dictated by the pixel size. The pixel size is dependent on the magnification used; for this work the pixel size is *ca.* 0.078 nm^2, corresponding to a further error of ca. 3.3% in volume for 50 nm NPs. Further errors will be introduced by defocusing rings and the ambiguity in particle extent arising from phase contrast with the support.

[28] V. Filipe, A. Hawe, W. Jiskoot, *Pharm. Res.* **2010**, *27*, 796–810.

[29] T. G. F. Souza, V. S. T. Ciminelli, N. D. S. Mohallem, *J. Phys. Conf. Ser.* **2016**, *733*, 012039.

[30] J. Stetefeld, S. A. McKenna, T. R. Patel, *Biophys. Rev.* **2016**, *8*, 409–427.